Systems metabolic engineering of *Corynebacterium glutamicum* for efficient L-tryptophan production

Yufei Dong[1], Zhen Chen[1,2]*

[1]Key Laboratory of Industrial Biocatalysis (Ministry of Education), Department of Chemical Engineering, Tsinghua University, Beijing 100084, China

[2]Center for Synthetic and Systems Biology, Tsinghua University, Beijing 100084, China

***Correspondence**

Corresponding author: Zhen Chen

E-mail: zhenchen2013@mail.tsinghua.edu.cn

Tel: +86-10-62772130. Fax: +86-10-62792128

Abstract:

Corynebacterium glutamicum is a versatile industrial microorganism for producing various amino acids. However, there have been no reports of well-defined *C. glutamicum* strains capable of hyperproducing L-tryptophan. This study presents a comprehensive metabolic engineering approach to establish robust *C. glutamicum* strains for L-tryptophan biosynthesis, including: (1) identification of potential targets by enzyme-constrained genome-scale modeling; (2) enhancement of the L-tryptophan biosynthetic pathway; (3) reconfiguration of central metabolic pathways; (4) identification of metabolic bottlenecks through comparative metabolome analysis; (5) engineering of the transport system, shikimate pathway, and precursor supply; and (6) repression of competing pathways and iterative optimization of key targets. The resulting *C. glutamicum* strain achieved a remarkable L-tryptophan titer of 50.5 g/L in 48h with a yield of 0.17 g/g glucose in fed-batch fermentation. This study highlights the efficacy of integrating computational modeling with systems metabolic engineering for significantly enhancing the production capabilities of industrial microorganisms.

Key word: L-tryptophan, *Corynebacterium glutamicum*, Metabolic engineering, Transporter engineering, Genome-scale modeling.

1. Introduction

L-tryptophan is an essential amino acid for both animals and human, which plays vital roles in protein synthesis and metabolic regulation. L-tryptophan and its derivatives [1], such as 5-hydroxy-L-tryptophan [2,3], violacein [4,5], indigos [6,7], and halogenated tryptophan [8,9], are extensively utilized in the pharmaceutical, cosmetic, food, and animal feed industries. Currently, the primary method for L-tryptophan production is microbial fermentation. In particular, metabolic engineering of *Escherichia coli* for the production of L-tryptophan has been intensively studied over the past few years, establishing *E. coli* as the predominant microbial chassis for industrial L-tryptophan production. Much of these research has focused on optimizing the rate-limiting steps in the L-tryptophan synthesis pathway, enhancing the availability of metabolic precursors such as phosphoenolpyruvate (PEP) and erythrose-4-phosphate (E4P), and blocking competing pathways and the L-tryptophan degradation pathway [10-14]. Furthermore, the development of riboswitch-based biosensors has facilitated the identification of new genetic targets to enhance L-tryptophan production [15]. By integrating various strategies, engineered *E. coli* strains have achieved L-tryptophan production titers of 40 to 55 g/L and yields of 0.15 to 0.23 g/g glucose in fed-batch fermentation [12,13,16]. However, compared to other amino acids such as L-lysine and L-threonine, the titers and yields of L-tryptophan achieved thus far remain relatively low, substantially below the theoretical yield of L-tryptophan. This discrepancy results in elevated production costs, thereby constraining the broader industrial utilization of L-tryptophan. Accordingly, the development of more robust and efficient microbial strains for L-tryptophan production is highly desirable.

Corynebacterium glutamicum is another important industrial chassis broadly used for the industrial production of amino acids [17,18]. It offers several advantages over *E. coli* for large-scale amino acid production, including enhanced safety, greater robustness to environmental stress, increased resistance to phage contamination, and the capacity to utilize a wide range of substrates [18-20]. Systems metabolic engineering strategies have been employed to engineer *C. glutamicum* microbial cell factories for the high-level production of L-lysine, L-arginine, L-proline, etc [21-26]. Early efforts to establish L-tryptophan production in *C. glutamicum* during the 1990s employed a strategy combining random mutagenesis with a limited number of rational genetic modifications [27]. This approach resulted in a strain achieving a record L-tryptophan titer of 58 g/L in fed-batch fermentation, highlighting the potential of *C. glutamicum* for high-level production of this amino acid. However, the engineered *C. glutamicum* strain exhibited several limitations, including retarded cell growth and low productivity, potentially attributed to the accumulation of deleterious mutations during repeated rounds of mutagenesis. Furthermore, the strain's reliance on a large plasmid and the requirement for exogenous L-phenylalanine and L-tyrosine supplementation hindered its suitability for industrial-scale applications. Therefore, the development of a genetically stable and well-defined *C. glutamicum* strain capable of hyperproducing L-tryptophan remains a priority.

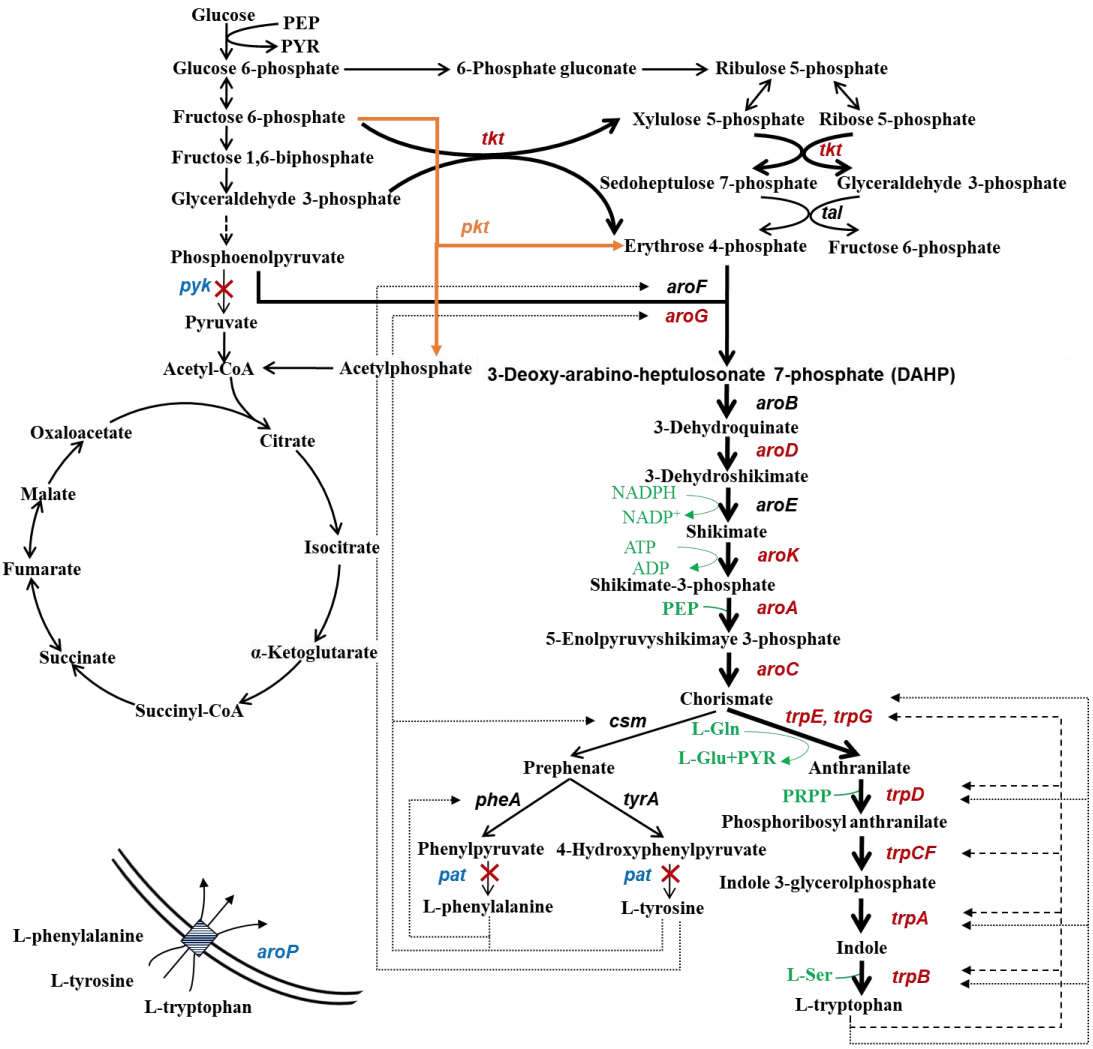

Fig. 1. Systematic metabolic engineering of *C. glutamicum* for L-tryptophan production. The dotted lines and dashed lines indicate feedback inhibition and repression, respectively. Precursors and cofactors are colored in green. The overexpression targets are shown with thick lines and red characters. The deletion or down-regulation targets are shown with thin lines and blue characters. The symbol "X" indicates gene deletion. The introduced exogenous phosphoketolase is colored in orange. PEP, phosphoenolpyruvate; PYR, pyruvate; L-Gln, L-glutamine; L-Ser, L-serine; PRPP, phosphoribosyl diphosphate.

In recent years, further elucidation of the crystal structures and functional mechanisms of the key enzymes for L-tryptophan synthesis, such as the chorismate mutase, the DAHP synthase [28], and the N-(5'-phosphoribosyl) anthranilate isomerase-indole-3-glycerol-phosphate synthase [29], has paved the way for the construction of L-tryptophan hyperproducing *C. glutamicum* strains. Moreover, development of novel L-tryptophan high-throughput screening platforms might facilitate large-scale target mining based on diversified libraries [30]. However, several challenges remain to be solved. Firstly, while the rate-limiting steps and metabolic regulation of L-tryptophan biosynthesis in *E. coli* have been extensively

studied, these aspects remain largely unexplored in *C. glutamicum*. Additionally, other potential metabolic engineering targets, such as L-tryptophan exporters or importers, have not been clearly elucidated in *C. glutamicum*. To address this knowledge gap, this study employed the integration of a genome-scale model (GEM) and omics analysis to identify potential metabolic targets. Subsequently, systems metabolic engineering strategies were implemented to engineer a wild-type *C. glutamicum* strain for enhanced L-tryptophan production (Fig. 1). These strategies involved debottlenecking the rate-limiting steps, balancing precursor supply, introducing novel L-tryptophan exporters, and repressing competing pathways. This comprehensive engineering approach enabled the construction of a well-defined *C. glutamicum* strain capable of producing L-tryptophan with a titer of 50.5 g/L in 48h with a yield of 0.17 g/g glucose in fed-batch fermentation, without using plasmids or supplementing other essential amino acids. This work lays the foundation for developing an economically viable process for industrial-scale L-tryptophan production.

2. Materials and methods

2.1. Bacterial strains and plasmids

The *C. glutamicum* strains used in this study are listed in Table 1. *E. coli* DH5α was used as the host for plasmid construction. The starting *C. glutamicum* strain MB001 was a prophage-free strain derived from ATCC 13032 [31]. The plasmids used in this study are listed in Table S1. The pK18*mobsacB*-derived plasmids were used for markerless gene deletion and integration in *C. glutamicum*. The pEC-K18*mob2* plasmid [32], an *E. coli* and *C. glutamicum* shuttle vector, was applied for gene overexpression in *C. glutamicum* strains.

2.2. Plasmids and strains construction

Gibson assembly was generally used for plasmid construction following the standard procedures. All of the primers used in this study are listed in Table S2. Gene deletion and insertion in *C. glutamicum* were conducted using the pK18*mobsacB*-derived plasmids through two rounds of recombination [33]. The codon-optimized phosphoketolase gene from *Bifidobacterium adolescentis* and the aromatic amino acid transporter genes were synthesized by Genewiz Company (Suzhou, China). The aromatic amino acid transporters tested in this study are listed in Table S3.

For the construction of plasmids for gene overexpression, the artificial promoter, the functional gene with a common a RBS (aaaggaggttgtc), and the rrnB terminator were inserted into the restriction sites EcoRI/XbaI of the plasmid pEC-K18*mob2* by Gibson assembly.

Table 1 Strains used in this study

Strains	Charateristics	Source
MB001	Prohage-free variant of *C. glutamicum*	Lab stock
TR01	MB001 with the substitution of promoter of *trp* operon by a strong promoter H36	This work
TR02	TR01, with point mutations in *trpD* (*trpD*$^{S149F/A162E}$)	This work
TR03	TR02 with genome integration of *aroG*^{D146N} from *E. coli* and *serA*$^{\Delta 197}$ from *C. glutamicum* under the control of *tuf* promoter	This work
TR04	TR03 with genome integration of *trpE*^{S40F}-*trpD* from *E. coli* under the control of *tuf* promoter at the intergenetic region between *cgp_1121* and *cgp_1122*	This work
TR05	TR04 with genome integration of *trpCBA* from *E. coli*	This work
TR06	TR05 with replacement of genome-integrated *trpD* from *E. coli* by *trp4* from *Saccharomyces cerevisiae*	This work
TR07	TR06 with deletion of *pyk*	This work
TR08	TR07 with insertion of a H36 promoter before *tkt* and change of *tkt* start codon from ttg to atg	This work
TR09	TR07 with genome integration of phosphoketolase gene mutant *pkt*$^{T2A/I6T/H260Y}$ from *Bifidobacterium adolescentis* under the control of *tuf* promoter into *bioA*	This work
TR10	TR07 with genome integration of phosphoketolase gene mutant *pkt*$^{T2A/I6T/H260Y}$ from *B. adolescentis* under the control of H36 promoter into *bioA*	This work
TR11	TR07 with genome integration of phosphoketolase gene from *B. adolescentis* under the control of *tuf* promoter into *bioA*	This work
TR12	TR07 with genome integration of phosphoketolase gene from *B. adolescentis* under the control of H36 promoter into *bioA*	This work
TR13	TR09 with deletion of *ldh*	This work
TR14	TR13 with genome integration of *yddG* from *Herbaspirillum rhizosphaerae* under the control of H36 promoter into *crtB2*	This work
TR15	TR13 with genome integration of *yddG* from *Paraburkholderia acidisoli* under the control of H36 promoter into *crtB2*	This work
TR16	TR13 with genome integration of *yddG* from *Herbaspirillum aquaticum* under the control of H36 promoter into *crtB2*	This work
TR17	TR13 with genome integration of *yddG* from *H. rhizosphaerae* under the control of *tuf* promoter into *crtB2*	This work
TR18	TR13 with genome integration of *yddG* from *P. acidisoli* under the control of *tuf* promoter into *crtB2*	This work
TR19	TR13 with genome integration of *yddG* from *H. aquaticum* under the control of *tuf* promoter into *crtB2*	This work
TR20	TR14 with genome intergration of *aroDC* from *C. glutamicum* under the control of H36 promoter into *crtI2*	This work

TR21	TR14 with genome intergration of *aroDC* from *C. glutamicum* under the control of *tuf* promoter into *crtI2*	This work
TR22	TR21 with genome integration of *glnA*^{E304A} from *Bacillus subtilis* and *prsA* from *C. glutamicum* MB001 under the control of H36 promoter into *crtYf*	This work
TR23	TR22 with genome integration of *tkt* from *C. glutamicum* under the control of H36 promoter into *bioD*	This work
TR24	TR23 with deletion of *pat*	This work
TR25	TR24 with deletion of *aroP*	This work
TR26	TR24 with genome integration of *aroG*^{D146N} from *E. coli* under the control of H36 promoter behind the genome-integrated *tkt* at the *bioD* locus	This work

2.3. Genome-scale metabolic modeling

To calculate the optimal metabolic flux distribution for biomass or L-tryptophan biosynthesis, flux balance analysis (FBA) was conducted based on the genome-scale enzyme-constrained model (ecCGL1) [34] of *C. glutamicum* using the CAVE platform [35]. The D-glucose uptake rate was set as 100, and the oxygen uptake rate was set as 1000 for aerobic condition. The objective product was selected as biomass or L-tryptophan.

To predict the specific metabolic engineering targets for L-tryptophan production, protein costs disparities between high growth low product generation (HGLP) (growth rate set as 0.46 h^{-1}) and low growth high product generation (LGHP) (growth rate set as 0.1 h^{-1}) situations were calculated based on ecCGL1 using ECMpy 2.0 [36]. The glucose uptake rate was set as 10 mmol·gDW^{-1} h^{-1}. Reactions with fold changes in enzyme costs over 1.5 between LGHP and HGLP conditions were selected as metabolic engineering targets [34]. The calculation was conducted in Python 3.12, and the code was obtained from the previous research [36].

2.4. Medium and culture conditions

For shake-flask fermentations, *C. glutamicum* strains were first cultured in 20 mL LSS1 medium in 250 mL baffled shake flasks at 30 °C, 200 rpm for 14-16 h [37]. The seed cultures were subsequently inoculated into 30 mL LPG2 medium in 500 mL baffled shake flasks with 30 g/L of $CaCO_3$ to perform L-tryptophan fermentations [38]. The initial concentration of glucose was 100 g/L. All shake-flask fermentations were conducted in duplicate at 30 °C, 200 rpm and an initial pH of 7.2. When necessary, 25 μg/L kanamycin was added.

Fed-batch fermentations were carried out in 5 L bioreactors containing 2 L LPG2 at

153 30 °C. The pH of the fermentation was kept at 7.0 with the automatic addition of 25%
154 (v/v) ammonia solution. The dissolved oxygen was maintained above 30% of air
155 saturation at an aeration rate of 2 L/min by adjusting the agitation speed. The feeding
156 solution containing 600 g/L glucose was fed to maintain the glucose concentration
157 lower than 10 g/L.

158 **2.5. Analysis of cell growth and extracellular metabolites**

159 Cell growth was detected by measuring the optical density of 600 nm (OD_{600}) of the
160 samples. The concentrations of glucose, lactic acid, and acetic acid were
161 quantitatively analyzed by high-performance liquid chromatography (HPLC)
162 equipped with an Aminex HPX-87H Column (300×7.8 mm) using 5 mM H_2SO_4 as
163 the mobile phase. The flow rate was set as of 0.8 mL/min at 65 °C and the injection
164 volume was 20 μL.

165 The concentrations of L-tryptophan were determined by HPLC with a Dikma
166 Diamonsil AAA Column (5μm, 250×4.6 mm) using the standard phenyl
167 isothiocyanate derivative method.[39] L-tryptophan was separated by using mobile
168 phase A (50 mM CH_3COONa, pH 6.5) and phase B (methanol: acetonitrile: water=1:
169 3: 1) with gradient elution at a total flow rate of 1 mL/min at 45 °C. The detective
170 wavelength was 254 nm and the injection volume was 10 μL.

171 **2.6. Metabolome analysis**

172 Intracellular metabolites in *C. glutamicum* cells were extracted as follows. Cells were
173 cultured to the exponential phase and 2 mL of each sample were taken. The cell
174 suspension was centrifuged at 4 °C, 12000 rpm for 1 min to remove the medium. The
175 cell pellets were washed gently with PBS buffer (pH=7.2-7.4) three times and the
176 supernatant was removed. Afterwards, 1.6 mL of pre-cooled (-80 °C) 80% methanol
177 was added immediately to resuspend the cell pellets by vortex. The samples were then
178 incubated at -20 °C for 30 min and processed by ultra-sonication for 2 min, followed
179 by incubation at -80 °C for 2 h for cell lysis. The suspension was subsequently
180 centrifuged at 4 °C, 14000 rpm for 15 min to remove the protein. The supernatant was
181 taken into a new 2 mL microcentrifuge tube, dried by vacuum and stored at -80 °C for
182 further operation.

183 The metabolites in the supernatant were analyzed by using SCIEXTriple Quad 6500+
184 liquid chromatography-tandem mass spectrometry (LC-MS/MS) system (AB Sciex,
185 Singapore) equipped with IonDrive detector and Qtrap-6500 mass spectrometer.

186 ## 3. Results and discussion

187 ### 3.1. Identification of potential engineering targets by genome-scale metabolic
188 modeling

189 As mentioned before, the metabolic regulation and rate-limiting reactions for
190 L-tryptophan biosynthesis in *C. glutamicum* have not been comprehensively
191 elucidated. Genome-scale metabolic modeling is a powerful tool for predicting
192 cellular phenotypes and serves as an invaluable approach for guiding metabolic
193 engineering strategies to enhance chemical production [40]. Recently, the first
194 enzyme-constrained model for *C. glutamicum*, ecCGL1, has been developed [34].
195 This model incorporates enzyme kinetic data and outperforms the widely used
196 stoichiometry-based model iCW773 in predicting phenotypes and identifying
197 engineering targets [34]. Therefore, we employed ecCGL1 to predict potential
198 engineering targets for L-tryptophan production.

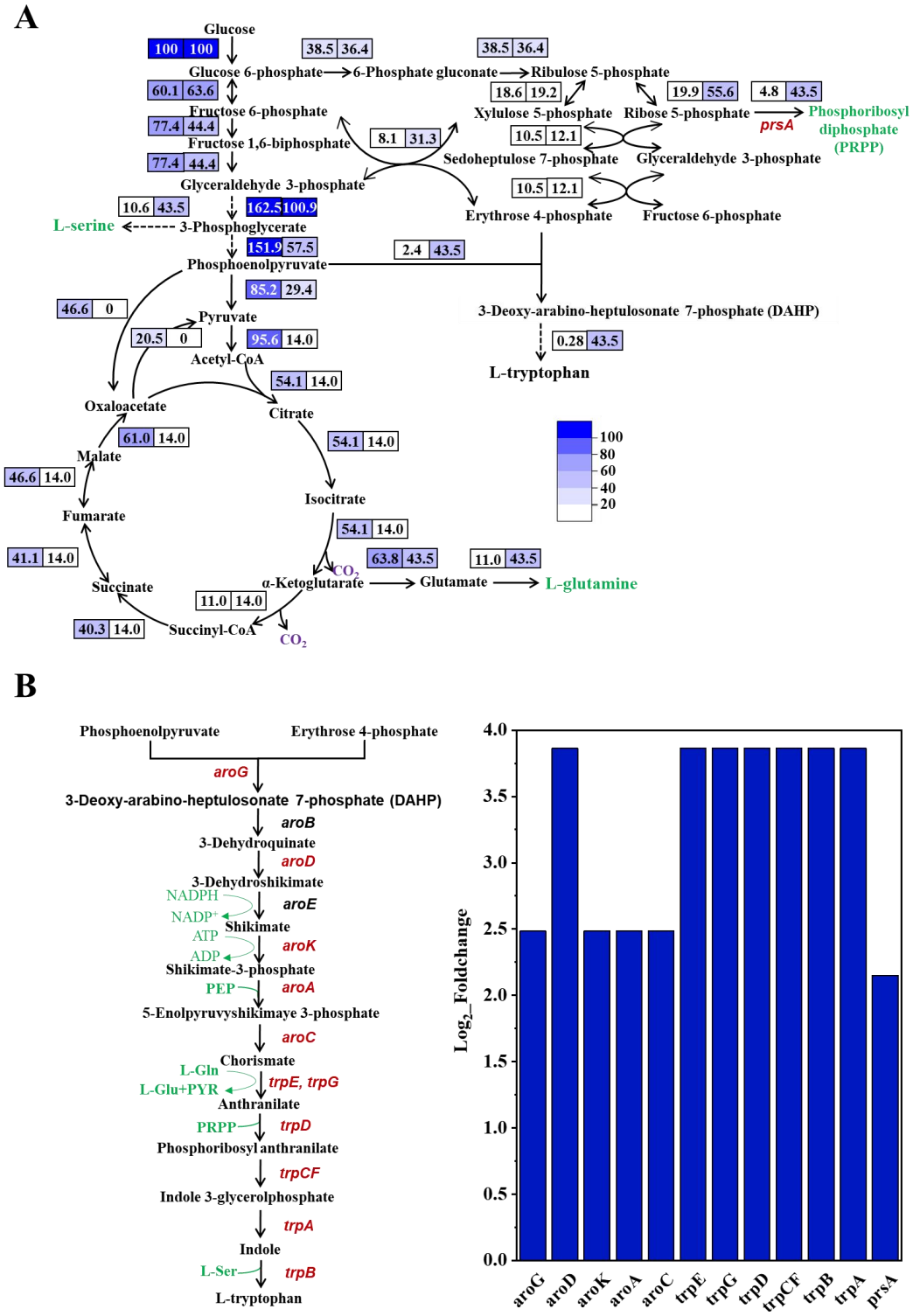

Fig. 2 Metabolic engineering targets prediction for L-tryptophan production by using the ecCGL1 model. (A) Metabolic flux distribution with the objective set as biomass accumulation (numbers on the left) and L-tryptophan production (numbers on the right). (B) Enhanced genetic targets identified by the approach of HGLP/LGHP. Precursors and cofactors are colored in green. The predicted targets are colored in red.

First, the theoretical yield of L-tryptophan and the optimized metabolic flux

206 distribution was calculated based on the stoichiometric data of ecCGL1 using the
207 CAVE platform [35]. As illustrated in Fig. 2A, the theoretical yield of L-tryptophan in
208 *C. glutamicum* is 0.435 mol/mol glucose, which is slightly higher than that in *E. coli*
209 (0.414 mol/mol glucose) [41]. To achieve the theoretical maximum yield of
210 L-tryptophan, the metabolic fluxes toward transketolase reaction involved in E4P
211 biosynthesis, the shikimate pathway, and the terminal steps of L-tryptophan
212 biosynthesis pathway must be significantly enhanced compared to those optimized for
213 cell growth (Fig. 2A). Moreover, the fluxes toward the biosynthesis of key metabolic
214 precursors, including L-serine, L-glutamine, and phosphoribosyl diphosphate (PRPP),
215 should also be increased (Fig. 2A). Conversely, the fluxes involved in the conversion
216 of PEP to pyruvate via the phosphotransferase system (PTS), PEP carboxylase, and
217 pyruvate kinase, as well as flux into tricarboxylic acid (TCA) cycle, must be
218 significantly reduced (Fig. 2A). These predicted results are generally consistent with
219 those previously implemented in *E. coli* [10-14], suggesting that the genome-scale
220 metabolic modeling is reliable.

221 While classical FBA based on stoichiometric balance could provide insights into
222 potential up- and down-regulated metabolic pathways, it cannot be used to identify
223 key targets within linear pathways. To overcome this limitation, we employed the
224 ecCGL1 model with the constraints of enzyme kinetic data to pinpoint crucial
225 enzymes based on protein cost discrepancies between HGLP and LGHP conditions
226 [36]. This analysis revealed twelve potential targets with >1.5-fold changes in enzyme
227 cost between HGLP and LGHP states (Fig. 2B and Table S4). These targets could be
228 functionally categorized into three modules: (1) genes (*trpE, trpG*, *trpD*, *trpCF*, *trpB,*
229 and *trpA*) encoding key enzymes within the terminal L-tryptophan biosynthesis
230 pathway, consistent with their roles in L-tryptophan overproduction [16,42]; (2)
231 shikimate pathway genes (*aroG*, *aroD*, *aroK, aroA*, *aroC*), similarly reported to be
232 important for L-tryptophan synthesis in *E. coli* [14]; (3) *prsA* gene encoding
233 ribose-phosphate diphosphokinase, responsible for catalyzing the synthesis of
234 L-tryptophan precursor PRPP. This study further elucidated the specific roles of these
235 genes in modulating L-tryptophan production in *C. glutamicum*.

236 **3.2. Enhancement of L-tryptophan synthesis pathway**

237 Genome-scale metabolic modeling indicated that enhanced expression of enzymes
238 within the shikimate and L-tryptophan biosynthetic pathways is crucial for increased
239 L-tryptophan production (Fig. 2B). To enhance the L-tryptophan synthesis pathway,
240 we initially attempted to increase the expression of the entire *trp* operon in *C.*
241 *glutamicum*. In *E. coli*, the *trp* operon is subject to both feedback repression by the
242 TrpR repressor and transcriptional attenuation mediated by the *trpL* leader sequence
243 (Fig. 3A). While *C. glutamicum* also utilizes *trpL*-mediated attenuation (Fig. 3A), a
244 TrpR homologue is absent in its genome. Therefore, to deregulate the *trp* operon in *C.*
245 *glutamicum* MB001, the native promoter was replaced with the strong constitutive
246 promoter H36, generating strain TR01. Shake-flask fermentation of TR01 yielded

247 only 0.15 g/L L-tryptophan, demonstrating that increased expression
248 of *trpEGDCFBA* alone is insufficient for substantial overproduction (Fig.
249 3B). Enzyme-constrained metabolic modeling revealed that anthranilate
250 phosphoribosyl transferase (TrpD) is required with high demand for L-tryptophan
251 biosynthesis (Fig. 2B). Furthermore, unlike its *E. coli* homologue, *C.*
252 *glutamicum* TrpD is subject to feedback inhibition by L-tryptophan (Fig. 1). To
253 alleviate this inhibition, point mutations S149F/A162E were introduced into TrpD of
254 strain TR01 [43], creating strain TR02. This modification significantly increased
255 L-tryptophan production to 2.70 g/L (Fig. 3B), establishing TrpD as a key control
256 point in *C. glutamicum* L-tryptophan biosynthesis. This contrasts with *E. coli*, where
257 the relief of feedback inhibition by L-tryptophan of anthranilate synthase subunit
258 TrpE rather than TrpD is significant for L-tryptophan production [44].

259 In addition to TrpD, the 3-deoxy-D-arabino-heptulosonate 7-phosphate (DAHP)
260 synthase, which catalyzes the condensation of PEP and E4P to DAHP, is another
261 critical enzyme controlling metabolic flux towards aromatic amino acid biosynthesis
262 (Fig. 2B). Given the feedback inhibition of the native DAHP synthases (AroG and
263 AroF) by aromatic amino acids [45], a feedback-resistant DAHP synthase variant,
264 $AroG^{D146N}$ from *E. coli* [46], was genomically integrated into strain TR02 under the
265 control of tuf promoter. Furthermore, to enhance the biosynthesis of the L-tryptophan
266 precursor L-serine, a copy of feedback-resistant D-3-phosphoglycerate dehydrogenase
267 gene $serA^{\Delta 197}$ from *C. glutamicum* [47] was also integrated after the heterogeneous
268 $aroG^{D146N}$ gene. The resulting strain TR03 exhibited an improved L-tryptophan
269 production of 3.37 g/L (Fig. 3B), suggesting that augmenting the supply of precursors
270 via the expression of feedback-resistant *aroG* and *serA* effectively promotes
271 L-tryptophan overproduction [27,48].

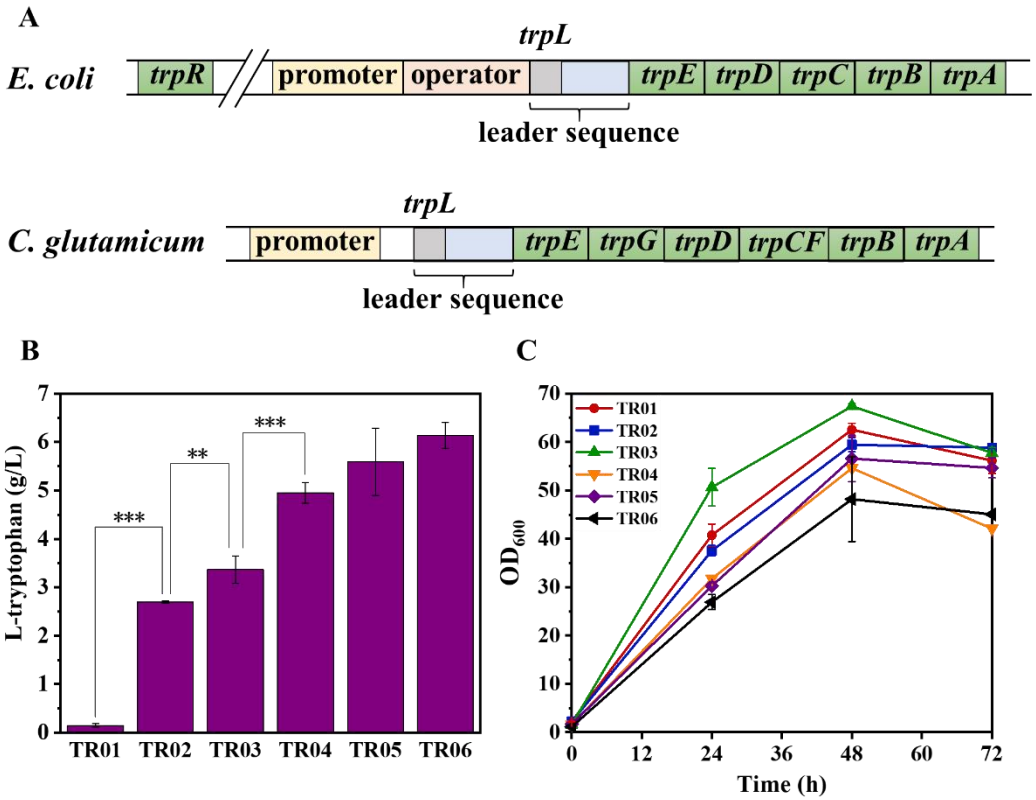

Fig. 3. Engineering of L-tryptophan biosynthesis pathway. (A) The *trp* operon in *E. coli* and *C. glutamicum*. (B) L-tryptophan production. (C) Cell growth. Two tailed t-tests indicate statistical significance compared to the parental strain. *P<0.1, **P<0.05, ***P<0.01.

To further enhance L-tryptophan production, we sought to optimize the L-tryptophan biosynthesis pathway as informed by enzyme-constrained metabolic modeling (Fig. 2B). Therefore, we attempted to integrated the *trpE*^{S40F}-*trpD*-*trpC*-*trpB*-*trpA* gene cluster from *E. coli* into strain TR03. Owing to the considerable size of the gene cluster (>6 kb) and the limited genome integration efficiency in *C. glutamicum*, the operon was divided into two fragments, specifically, *trpE*^{S40F}-*trpD* and *trpC*-*trpB*-*trpA*, and sequentially integrated into the genome of TR03 under the control of the *tuf* promoter, resulting in the generation of strains TR04 and TR05, respectively. The *trpE*^{S40F} encodes a feedback-resistant anthranilate synthase. The L-tryptophan production by both TR04 and TR05 was elevated, with strain TR05 achieving a titer of 5.60 g/L (Fig. 3B). Furthermore, given that TrpD was predicted to be a critical target within the L-tryptophan biosynthesis pathway (Fig. 2B), we sought to enhance its activity by incorporating a more efficient variant. Previous studies have reported that the TrpD from *Saccharomyces cerevisiae* encoded by *trp4* gene displays a higher affinity for PRPP and greater enzymatic activity compared to the TrpD from *E. coli* [49]. Consequently, we substituted the *E. coli*-derived *trpD* in TR05 with *trp4* from *S. cerevisiae*, yielding strain TR06. This modification resulted in a further increase in L-tryptophan production to 6.13 g/L (Fig. 3B), confirming its significant role for affecting L-tryptophan overproduction.

296 **3.3. Enhancement of PEP and E4P supply**

297 After optimizing the terminal L-tryptophan biosynthesis pathway, efforts were
298 directed towards enhancing the supply of PEP and E4P, the two direct precursors of
299 aromatic amino acids. To increase PEP availability, the *pyk* gene in strain TR06 was
300 deleted, thereby blocking the conversion of PEP to pyruvate via pyruvate kinase. The
301 resulting strain TR07 exhibited a 8.1% increase in L-tryptophan titer (Fig. 4A).
302 Additionally, an increase in both glucose consumption rate (Fig. S1) and L-tryptophan
303 synthesis rate (Fig. 4A) was observed, suggesting that elevating PEP supply positively
304 impacts glucose consumption through the PTS and L-tryptophan biosynthesis via
305 DAHP synthase.

306 To further augment E4P supply, two distinct strategies were employed. Initially, we
307 endeavored to boost transketolase activity in strain TR07 by inserting a strong H36
308 promoter upstream of the endogenous *tkt* gene and substituting its start codon from ttg
309 to atg. However, this modification did not yield an improvement in L-tryptophan yield
310 in the resulting strain TR08 (Fig. 4A). Consequently, an alternative E4P synthesis
311 pathway was explored by introducing a heterologous phosphoketolase. Previous
312 studies have demonstrated that the phosphoketolase from *Bifidobacterium*
313 *adolescentis* could efficiently convert fructose 6-phosphate (F6P) to E4P and
314 acetylphosphate [50], and this enzyme has been successfully applied to enhance
315 aromatic amino acid production [13]. Consequently, both the wild-type *pkt* gene and
316 its mutant variant $pkt^{T2A/I6T/H260Y}$, which encodes an enzyme with higher specific
317 activity [51], were introduced into strain TR07 under the control of either the *tuf* or
318 H36 promoters, generating strains TR09-TR12 (Fig. 4C). These strains exhibited
319 varied responses in terms of cell growth, L-tryptophan production, and lactate
320 accumulation (Fig. 4). Notably, strain TR09 demonstrated the most significant
321 improvement in L-tryptophan titer, showing a 8.4% increase over the control strain
322 TR07 (Fig. 4C). Furthermore, cell growth of TR09 was comparable to that of TR07
323 (Fig. 4D), while lactate accumulation was notably reduced (Fig. 4E). These findings
324 underscored the importance of optimizing *pkt* expression and phosphoketolase
325 activity to balance cell growth with L-tryptophan production. Given the observed
326 lactate accumulation during L-tryptophan production, the *ldh* gene encoding lactate
327 dehydrogenase was deleted in strain TR09. The resulting strain TR13 exhibited a
328 6.4% increase in L-tryptophan titer compared to TR09, with no detectable lactate
329 accumulation during fermentation (Fig. 4).

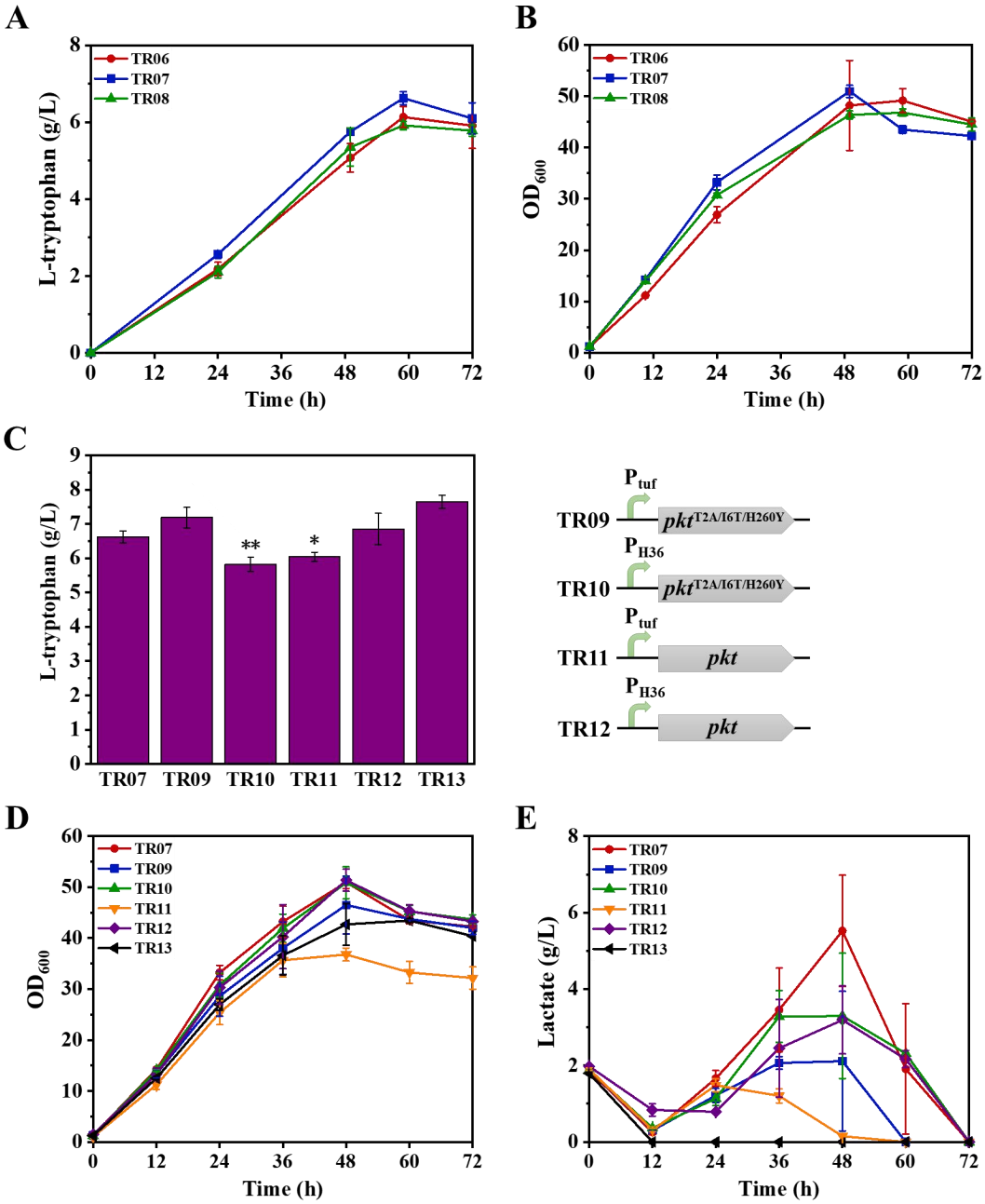

330

331 **Fig. 4. Engineering of the central metabolic pathways.** (A) L-tryptophan
332 production by strains TR07 and TR08. (B) Cell growth. (C) L-tryptophan production.
333 (D) Cell growth. (E) Lactate accumulation. Two tailed t-tests indicate statistical
334 significance compared to TR07. *P<0.1, **P<0.05, ***P<0.01.

335 **3.4. Metabolome analysis**

336 To elucidate alterations in cellular metabolism and potential bottlenecks hindering
337 L-tryptophan production, a comparative metabolome analysis was conducted between
338 the engineered strain TR13 and the wild-type strain MB001. This analysis focused on
339 central metabolic pathway intermediates and intracellular amino acids. As illustrated

in Fig. 5A, a total of 108 metabolites within central metabolic pathways were quantified, with significant increases observed in 27 metabolites and significant decreases in 18 metabolites within the TR13 strain (Table S5). Notably, most metabolites in the glycolysis pathway exhibited elevated concentrations in TR13, except for F6P. This exception is possibly due to the introduction of phosphoketolase, which results in the conversion of F6P to E4P. Moreover, the concentrations of PEP and most metabolites in the pentose phosphate pathway were elevated, indicating no apparent supply limitation of PEP and E4P (Fig. S2). Importantly, the concentration of shikimate in TR13 increased by 156-fold, indicating that optimizing the downstream portion of the shikimate pathway to reduce shikimate accumulation is essential for improving L-tryptophan production.

Regarding the change in intracellular amino acids, TR13 showed significant increases in 5 amino acids and decreases in 4 amino acids compared to MB001 (Fig. 5B and Table S5). In particular, the intracellular levels of L-tryptophan and L-tyrosine in TR13 were elevated by 170-fold and 12.4-fold, respectively. This suggests that enhancing L-tryptophan export and reducing L-tyrosine biosynthesis could be potential strategies for increasing L-tryptophan production. Conversely, a pronounced decrease in the concentrations of L-glutamine and PRPP was observed in TR13, indicating that increasing the availability of these two precursors may be necessary to boost L-tryptophan production. It was also noticed that the concentration of lactate dramatically reduced in TR13 due to deletion of the *ldh* gene. Overall, this metabolome analysis provided new targets for further enhancing L-tryptophan production.

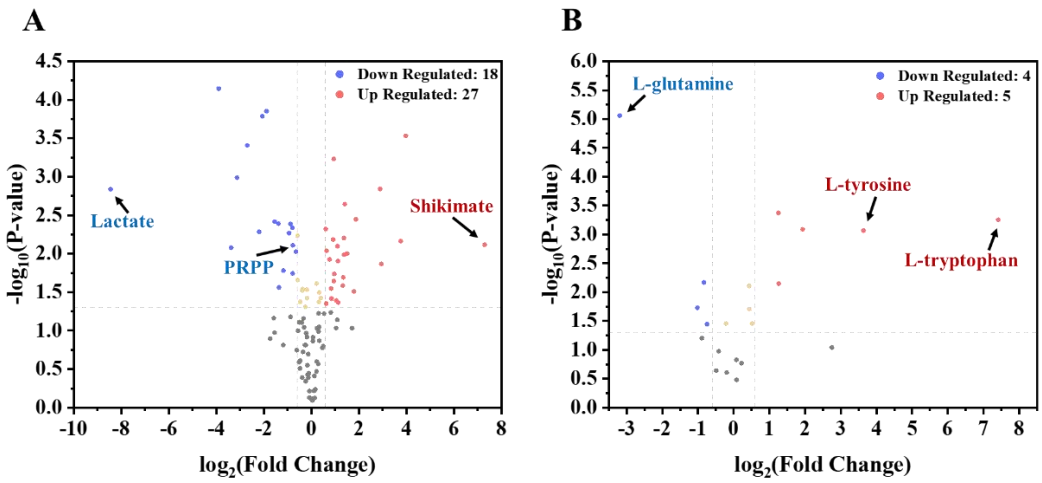

Fig. 5. Comparative metabolome analysis of TR13 and MB001. (A) Volcano plot depicting changes of intracellular metabolites within central metabolic pathways. (B) Volcano plot depicting changes of intracellular amino acids. Metabolites with average fold change ≥1.5, t-test p ≤0.05 were considered significantly different.

368 **3.5. Transporter engineering to increase L-tryptophan production**

369 The metabolome analysis revealed a substantial accumulation of intracellular
370 L-tryptophan in strain TR13. Consequently, enhancing the export of L-tryptophan
371 could mitigate its cellular toxicity and alleviate the feedback inhibition imposed on
372 enzymes in the L-tryptophan biosynthesis pathway. Given that no endogenous
373 L-tryptophan exporter has been identified in *C. glutamicum*, we employed
374 PSI-BLAST to identify potential L-tryptophan exporters in the Uniprot database,
375 using the sequence of the *E. coli* L-tryptophan exporter YddG as a query [15]. Seven
376 candidate exporters were selected (Table S3), and the corresponding genes were
377 subsequently overexpressed in strain TR13 with plasmid pEC-K18*mob2* (Fig. 6A).
378 Strains overexpressing *yddG* from *Herbaspirillum rhizosphaerae* (Hrh),
379 *Herbaspirillum aquaticum* (Haq), and *Paraburkholderia acidisoli* (Pac) exhibited the
380 most significant increase in L-tryptophan titers (Fig. 6A). Subsequently, the three
381 selected *yddG* genes were individually integrated into the genome of strain TR13
382 under the control of either the H36 or *tuf* promoter, resulting in the generation of
383 strains TR14 to TR19 (Fig. 6C). All engineered strains demonstrated a
384 substantial increase in L-tryptophan titer (Fig. 6C) without compromising cellular
385 growth (Fig. 6B). Specifically, strain TR14, harboring the integrated *H. rhizosphaerae*
386 *yddG* gene under the H36 promoter, achieved the highest L-tryptophan titer of 11.24
387 g/L, which is improved by 80.7% compared with strain TR13 (Fig. 6C). These
388 findings suggest that L-tryptophan export represents a critical bottleneck in
389 L-tryptophan production in *C. glutamicum*. Therefore, screening for and optimizing
390 the expression of appropriate *yddG* genes is essential for enhancing L-tryptophan
391 production in this organism.

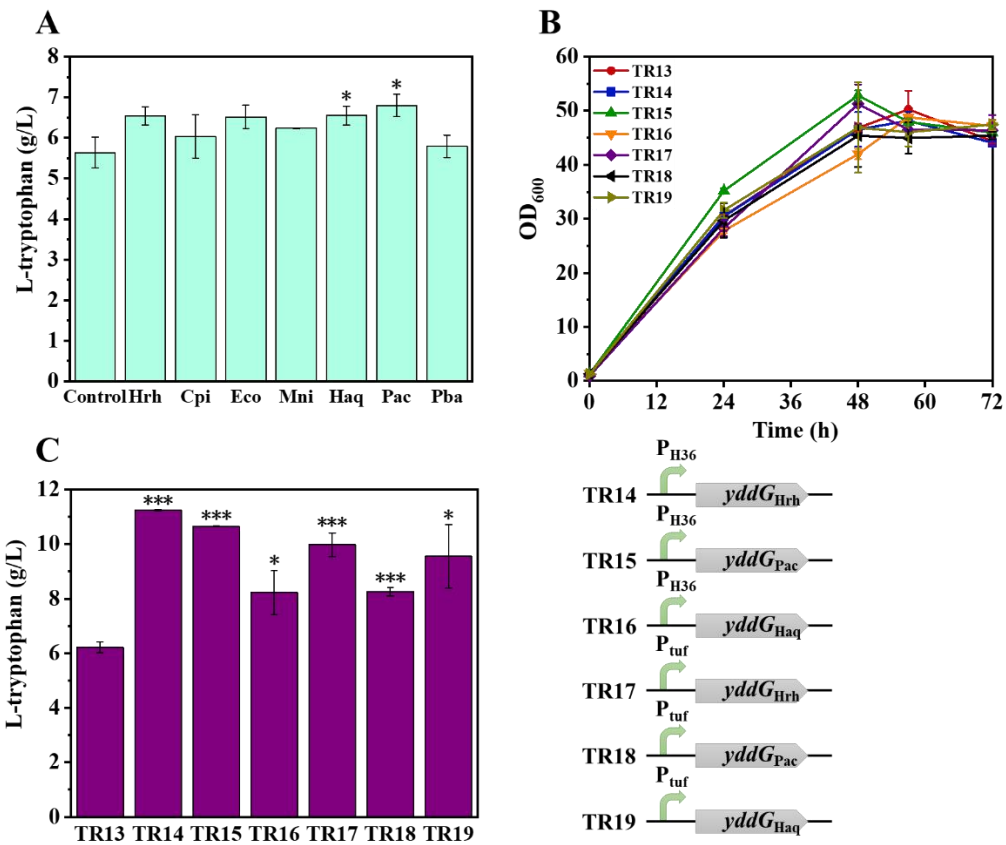

Fig. 6. Screening of L-tryptophan exporters. (A) Screening of potential L-tryptophan exporters with plasmid pEC-K18*mob2*. The control group contained an empty pEC-K18*mob2* plasmid. (B) Cell growth of the engineered strains. (C) L-tryptophan production by strains with integrated L-tryptophan exporters in genome. Two tailed t-tests indicate statistical significance compared to the control group or strain TR13. *P<0.1, **P<0.05, ***P<0.01.

3.6. Optimization of the shikimate pathway

Given the significant accumulation of shikimate observed in the metabolome analysis of strain TR13 (Fig. 5), it is necessary to optimize the shikimate pathway to redirect metabolic flux toward L-tryptophan production. Enzyme-constrained metabolic modeling indicated that the genes *aroD*, *aroK*, *aroA*, and *aroC* are potential targets within the shikimate pathway (Fig. 2B). To investigate this prediction, each of these genes was individually overexpressed in strain TR13 with plasmid pEC-K18*mob2*. Overexpression of *aroA* did not significantly impact L-tryptophan production, while *aroK* overexpression resulted in a decrease in L-tryptophan titer (Fig. 7A). Conversely, overexpression of either *aroC* or *aroD* led to a 15.8% increase in L-tryptophan titer (Fig. 7A), suggesting that the native expression levels of these genes may limit L-tryptophan biosynthesis in *C. glutamicum*. To further validate the general applicability of these findings, the *aroD* and *aroC* genes were simultaneously integrated into the genome of strain TR14 under the control of either the H36 or tuf

promoter, resulting in the creation of strains TR20 and TR21, respectively. Both TR20 and TR21 demonstrated enhanced L-tryptophan production, with strain TR21 achieving the highest titer, a 20.1% improvement compared to the parental strain TR14 (Fig. 7B). Additionally, cell growth of TR20 and TR21 was not negatively affected (Fig. 7C).

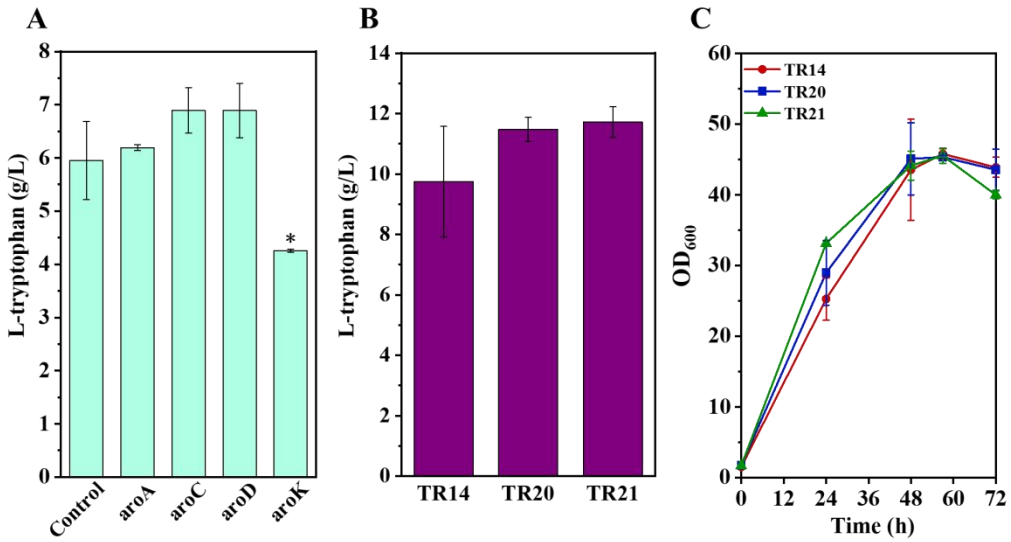

Fig. 7. Optimization of the shikimate pathway. (A) L-tryptophan production by strains overexpressing *aroA*, *aroC*, *aroD*, and *aroK* genes. (B) L-tryptophan production by simultaneously overexpressing *aroD-aroC* genes. (C) Cell growth of the engineered strains. Two tailed t-tests indicate statistical significance compared to the control group. *P<0.1, **P<0.05, ***P<0.01.

3.7. Optimization of the availability of other precursors

Metabolome analysis revealed significantly reduced intracellular concentrations of L-glutamine and PRPP in TR13(Fig. 5), suggesting that increasing the availability of these precursors may enhance L-tryptophan production. To increase the supply of L-glutamine and PRPP, four *glnA* genes encoding glutamine synthetases and three *prsA* genes encoding PRPP synthetase from various organisms (Table S6), which were characterized with high enzymatic activities [52], were individually overexpressed in strain TR14 with plasmid pEC-K18*mob2*. All strains overexpressing *glnA* exhibited increased L-tryptophan production while those overexpressing *prsA* from *E. coli* or *C. glutamicum* also demonstrated elevated L-tryptophan titers (Fig. 8A). The most significant improvements were observed in strains overexpressing the feedback-resistant $glnA^{E304A}$ from *Bacillus subtilis* [53] and the native *prsA* from *C. glutamicum* (Fig. 8A). Consequently, the $glnA^{E304A}$ gene from *B. subtilis* and the *prsA* gene from *C. glutamicum* were co-integrated into the genome of TR21, creating strain TR22. The L-tryptophan titer by strain TR22 was increased to 12.0 g/L, and the yield was increased from 0.108 to 0.115 g/g glucose, representing a 6.5% improvement

compared to strain TR21 (Fig. 8B). Moreover, the cell growth of TR22 was also improved (Fig. 8C).

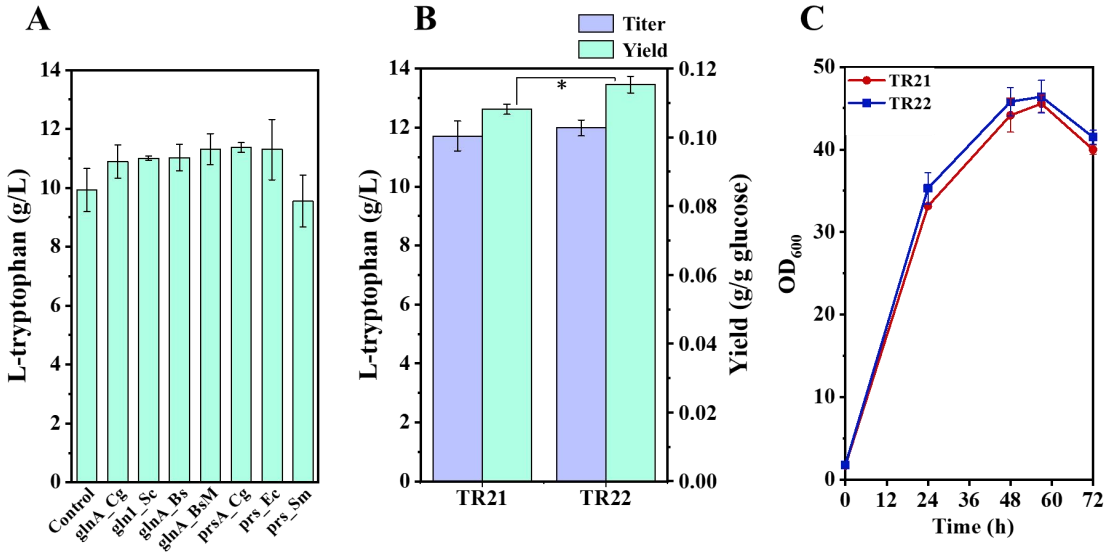

Fig. 8. Increasing of the supply of glutamine and PRPP to enhance L-tryptophan production. (A) L-tryptophan production by strains overexpressing glutamine synthetase and PRPP synthetase genes. (B) L-tryptophan production by simultaneously overexpressing *glnA*_BsM-*prsA*_Cg genes. (C) Cell growth of the engineered strains. Two tailed t-tests indicate statistical significance. *P<0.1, **P<0.05, ***P<0.01.

3.8. Iterative optimization of key targets and knockdown of competing pathways

Although the production of L-tryptophan by strain TR22 was significantly enhanced through the integration of various metabolic engineering strategies, the resulting titer remains insufficient for industrial application. Recognizing that new bottlenecks may emerge during the engineering process, an iterative optimization approach was employed to fine-tune the supply of precursors and the L-tryptophan biosynthesis pathway. First, to ensure an adequate supply of E4P, an additional copy of the *tkt* gene under the control of the H36 promoter was integrated into the genome of TR22, generating strain TR23. The production of L-tryptophan by strain TR23 increased to 13.7 g/L (Fig. 9A), indicating that E4P shortage had emerged during the construction of strain TR22.

Subsequently, to reduce the metabolic flux toward the biosynthesis of other aromatic amino acids, the *pat* gene encoding prephenate aminotransferase was deleted in TR23. The resulting strain TR24 exhibited a further increase in L-tryptophan titer to 15.4 g/L (Fig. 9A). Notably, the cell growth of strain TR24 was unaffected (Fig. 9B), which could be due to the existence of other non-specific aminotransferases that can compensate for the synthesis of L-phenylalanine and L-tyrosine [54-56]. To block

467 L-tryptophan uptake, the aromatic amino acid importer gene *aroP* [57] was deleted in
468 strain TR24, generating strain TR25. However, this modification resulted in a slight
469 reduction in L-tryptophan titer (Fig. 9A) as well as decreased glucose consumption
470 rate (Fig. 9C), indicating the import of L-tryptophan is not a limiting factor for
471 L-tryptophan production in *C. glutamicum*.

472 In an effort to further increase flux through the shikimate pathway, an additional copy
473 of $aroG^{D146N}$ from *E. coli* was integrated into the genome of strain TR24. The
474 resulting strain TR26 showed an improved L-tryptophan titer of 16.2 g/L (Fig. 9A)
475 with a yield of 0.16 g/g glucose, which is comparable to the reported yield in *E. coli*.
476 These findings underscore the necessity of iterative optimization in strain engineering
477 to address emerging bottlenecks and achieve higher product titers.

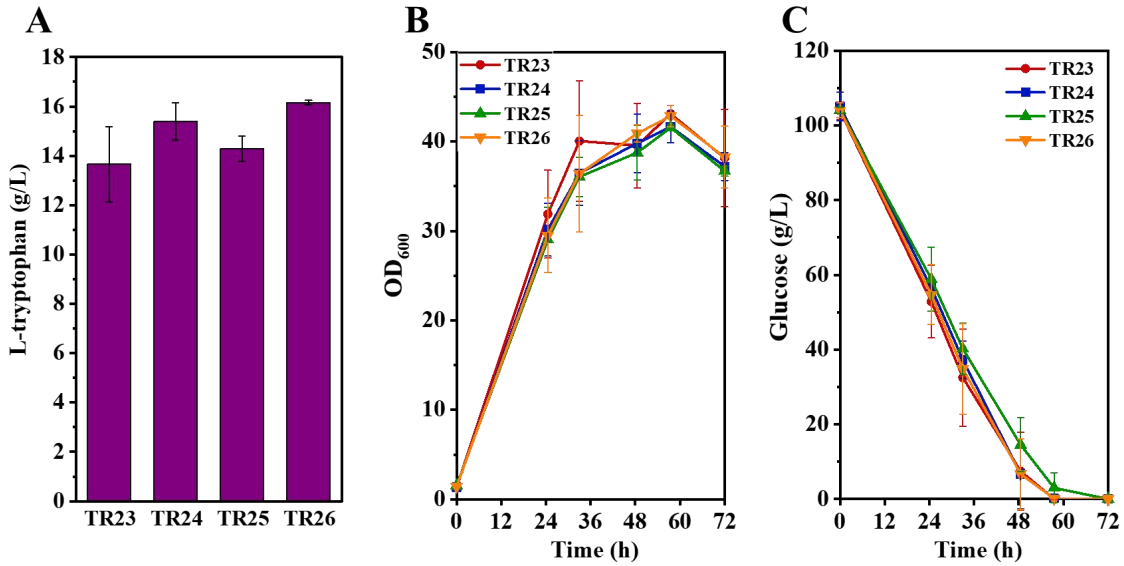

478

479 **Fig. 9. Iterative optimization of the L-tryptophan-producing strain.** (A)
480 L-tryptophan production of the engineered strains. (B) Cell growth of the engineered
481 strains. (C) Glucose uptake of the engineered strains.

482 **3.9. Fed-batch production of L-tryptophan**

483 Fed-batch fermentations of strain TR26 were conducted in 5 L bioreactors to assess its
484 potential for large-scale production of L-tryptophan. L-tryptophan was gradually
485 accumulated during the fermentation process and finally reached a titer of 50.5 g/L at
486 48 h with a yield of 0.17 g/g glucose (Fig. 10). The obtained titer and yield of
487 L-tryptophan were comparable to the highest levels reported in *E. coli* strains [11-16].
488 Notably, the biomass of strain TR26 was continuously increased to a high OD_{600} of
489 approximately 280 during the fed-batch fermentation, which might compete with the
490 synthesis of L-tryptophan. Therefore, further genomic modification of strain TR26 to
491 reduce biomass accumulation as well as medium and process optimization could be
492 explored to further increase the titer and yield of L-tryptophan.

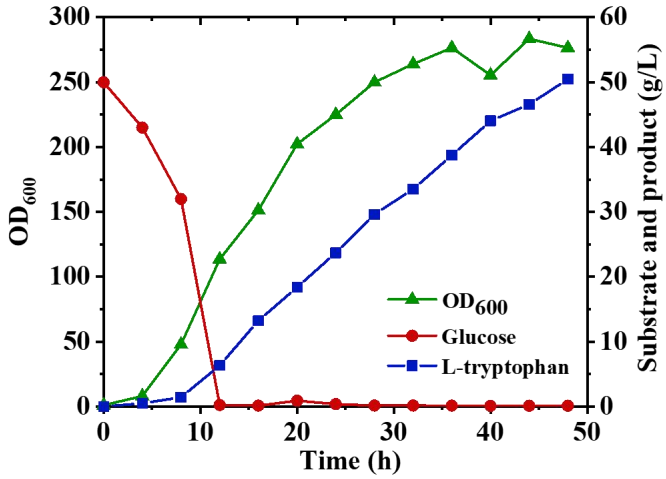

Fig. 10. Fed-batch fermentation of strain TR26 in 5 L bioreactor.

4. Conclusion

In conclusion, this study successfully engineered L-tryptophan-overproducing *C. glutamicum* strains with a defined genetic background using a systems metabolic engineering approach. By integrating enzyme-constrained genome-scale metabolic modeling (ecCGL1) and comparative metabolome analysis, a series of key targets for enhancing L-tryptophan biosynthesis, including *trpD*, *aroC*, *aroD*, and others, were identified, highlighting differences in metabolic regulation compared to *E. coli*. Furthermore, the overexpression of heterologous phosphoketolase, glutamine synthetases, and PRPP synthetase, coupled with the optimization of selected L-tryptophan exporters, significantly improved precursor supply and export efficiency, leading to a substantial increase in L-tryptophan titer. Through iterative rounds of model-guided engineering and metabolome analysis, a final strain capable of producing 16.2 g/L of L-tryptophan with a yield of 0.16 g/g glucose in shake-flask fermentations was obtained. Fed-batch fermentations of this strain led to an L-tryptophan titer of 50.5 g/L in 48h with a yield of 0.17 g/g glucose, which was comparable to the best reported *E. coli* producers. Notably, the engineered strain is plasmid-free and devoid of unknown mutations, representing a promising platform for industrial L-tryptophan production. Future efforts to further enhance L-tryptophan production can be directed towards the exploration of additional potential targets through multi-omics analysis and the optimization of fermentation processes.

Declaration of interests

None.

Acknowledgments

This work was supported by the National Key R&D Program of China (No. 2021YFC2100900), the National Natural Science Foundation of China (Grant Nos. 21938004, 22078172), and Tsinghua University Initiative Scientific Research Program (No. 20223080016).

Author Contributions

Yufei Dong: Methodology, Investigation, Formal analysis, Data curation, Validation, Writing-original draft preparation. Zhen Chen: Conceptualization, Investigation, Formal analysis, Writing - original draft, Writing - review & editing, Funding acquisition, Resources, Supervision, Project administration.

6 Reference

[1] Xiao S, Wang Z, Wang B, Hou B, Cheng J, Bai T, et al. Expanding the application of tryptophan: Industrial biomanufacturing of tryptophan derivatives. Front Microbiol 2023;14:1099098. https://doi.org/10.3389/fmicb.2023.1099098.

[2] Lee J, Lee J. Recent research progress in the microbial production of aromatic compounds derived from L-tryptophan. J Life Sci 2020;30(10):919-29. https://doi.org/10.5352/JLS.2020.30.10.919

[3] Shen YP, Niu FX, Yan ZB, Fong LS, Huang YB, Liu JZ. Recent advances in metabolically engineered microorganisms for the production of aromatic chemicals derived from aromatic amino acids. Front Bioeng Biotechnol 2020;8:407. https://doi.org/10.3389/fbioe.2020.00407.

[4] Sarwar N, Sarwar S, Ejaz S, Al-Adeeb A, Al-Ansi W, Li Y, et al. Metabolic engineering of microorganisms to increase production of violacein. Int J Agric Environ Biotechnol 2021;6(1):295-306. https://doi.org/10.22161/ijeab.61.37.

[5] Füller JJ, Röpke R, Krausze J, Rennhack KE, Daniel NP, Blankenfeldt W, et al. Biosynthesis of violacein, structure and function of l-tryptophan oxidase VioA from *Chromobacterium violaceum*. J Biol Chem 2016;291(38):20068-84. https://doi.org/10.1074/jbc.M116.741561.

[6] Choi KY. A review of recent progress in the synthesis of bio-indigoids and their biologically assisted end-use applications. Dyes Pigm 2020;181:108570. https://doi.org/10.1016/j.dyepig.2020.108570.

[7] Cao M, Gao M, Suástegui M, Mei Y, Shao Z. Building microbial factories for the production of aromatic amino acid pathway derivatives: From commodity chemicals to plant-sourced natural products. Metab Eng 2020;58:94-132. https://doi.org/10.1016/j.ymben.2019.08.008.

558 [8] Kerbs A, Burgardt A, Veldmann KH, Schäffer T, Lee JH, Wendisch VF. Fermentative
559 production of halogenated tryptophan derivatives with *Corynebacterium glutamicum*
560 overexpressing tryptophanase or decarboxylase genes. Chembiochem
561 2022;23(9):e202200007. https://doi.org/10.1002/cbic.202200007.
562 [9] Veldmann KH, Minges H, Sewald N, Lee J-H, Wendisch VF. Metabolic engineering of
563 *Corynebacterium glutamicum* for the fermentative production of halogenated
564 tryptophan. J Biotechnol 2019;291(10):7-16.
565 https://doi.org/10.1016/j.jbiotec.2018.12.008.
566 [10] Chen L, Zeng AP. Rational design and metabolic analysis of *Escherichia coli* for effective
567 production of L-tryptophan at high concentration. Appl Microbiol Biotechnol
568 2016;101(2):559-68. https://doi.org/10.1007/s00253-016-7772-5.
569 [11] Wang J, Cheng LK, Wang J, Liu Q, Shen T, Chen N. Genetic engineering of *Escherichia*
570 *coli* to enhance production of l-tryptophan. Appl Microbiol Biotechnol
571 2013;97(17):7587-96. https://doi.org/10.1007/s00253-013-5026-3.
572 [12] Guo L, Ding S, Liu Y, Gao C, Hu G, Song W, et al. Enhancing tryptophan production by
573 balancing precursors in *Escherichia coli*. Biotechnol Bioeng 2021;119(3):983-93.
574 https://doi.org/10.1002/bit.28019.
575 [13] Xiong B, Zhu Y, Tian D, Jiang S, Fan X, Ma Q, et al. Flux redistribution of central carbon
576 metabolism for efficient production of l-tryptophan in *Escherichia coli*. Biotechnol Bioeng
577 2021;118(3):1393-404. https://doi.org/10.1002/bit.27665.
578 [14] Liu S, Wang B-B, Xu JZ, Zhang WG. Engineering of shikimate pathway and terminal
579 branch for efficient production of L-tryptophan in *Escherichia coli*. Int J Mol Sci
580 2023;24(14):11866. https://doi.org/10.3390/ijms241411866.
581 [15] Tang M, Pan X, Yang T, You J, Zhu R, Yang T, et al. Multidimensional engineering of
582 *Escherichia coli* for efficient synthesis of L-tryptophan. Bioresour Technol
583 2023;386:129475. https://doi.org/10.1016/j.biortech.2023.129475.
584 [16] Niu H, Li R, Liang Q, Qi Q, Li Q, Gu P. Metabolic engineering for improving l-tryptophan
585 production in *Escherichia coli*. J Ind Microbiol Biotechnol 2019;46(1):55-65.
586 https://doi.org/10.1007/s10295-018-2106-5.
587 [17] Bampidis V, Azimonti G, de Lourdes Bastos M, Christensen H, Dusemund B, Kouba M, et
588 al. Safety and efficacy of l-tryptophan produced by fermentation with
589 *Corynebacterium glutamicum* KCCM 80176 for all animal species. EFSA J
590 2019;17(6):e05729. https://doi.org/10.2903/j.efsa.2019.5729.
591 [18] Zha J, Zhao Z, Xiao Z, Eng T, Mukhopadhyay A, Koffas MAG, et al. Biosystem design of
592 *Corynebacterium glutamicum* for bioproduction. Curr Opin Biotechnol 2023;79.
593 https://doi.org/10.1016/j.copbio.2022.102870.
594 [19] Chai M, Deng C, Chen Q, Lu W, Liu Y, Li J, et al. Synthetic biology toolkits and metabolic
595 engineering applied in *Corynebacterium glutamicum* for biomanufacturing. ACS Synth
596 Biol 2021;10(12):3237-50. https://doi.org/10.1021/acssynbio.1c00355.
597 [20] Unthan S, Baumgart M, Radek A, Herbst M, Siebert D, Brühl N, et al. Chassis organism
598 from *Corynebacterium glutamicum*-a top-down approach to identify and delete
599 irrelevant gene clusters. Biotechnol J 2014;10(2):290-301.
600 https://doi.org/10.1002/biot.201400041.
601 [21] Kogure T, Inui M. Recent advances in metabolic engineering of *Corynebacterium*

602 *glutamicum* for bioproduction of value-added aromatic chemicals and natural products.
603 Appl Microbiol Biotechnol 2018;102(20):8685-705.
604 https://doi.org/10.1007/s00253-018-9289-6.
605 [22] Liu J, Xu JZ, Rao ZM, Zhang WG. Industrial production of L-lysine in *Corynebacterium*
606 *glutamicum*: Progress and prospects. Microbiol Res 2022;262:127101.
607 https://doi.org/10.1016/j.micres.2022.127101.
608 [23] Zhao Z, Cai M, Liu Y, Hu M, Yang F, Zhu R, et al. Genomics and transcriptomics-guided
609 metabolic engineering *Corynebacterium glutamicum* for l-arginine production.
610 Bioresour Technol 2022;364:128054. https://doi.org/10.1016/j.biortech.2021.125799.
611 [24] Jiang Y, Sheng Q, Wu XY, Ye BC, Zhang B. L-arginine production in *Corynebacterium*
612 *glutamicum*: manipulation and optimization of the metabolic process. Crit Rev
613 Biotechnol 2021;41(2):172-85. https://doi.org/10.1080/07388551.2020.1844625.
614 [25] Zhang J, Qian F, Dong F, Wang Q, Yang J, Jiang Y, et al. De novo engineering of
615 *Corynebacterium glutamicum* for l-Proline production. ACS Synth Biol
616 2020;9(7):1897-906. https://doi.org/10.1021/acssynbio.0c00249.
617 [26] Liu J, Liu M, Shi T, Sun G, Gao N, Zhao X, et al. CRISPR-assisted rational flux-tuning and
618 arrayed CRISPRi screening of an l-proline exporter for l-proline hyperproduction. Nat
619 Commun 2022;13(1):891. https://doi.org/10.1038/s41467-022-28501-7.
620 [27] Ikeda M, Katsumata R. Hyperproduction of tryptophan by *Corynebacterium glutamicum*
621 with the modified pentose phosphate pathway. Appl Environ Microbiol 1999;65(6):2497–
622 502. https://doi.org/10.1128/AEM.65.6.2497-2502.1999.
623 [28] Burschowsky D, Thorbjørnsrud HV, Heim JB, Fahrig-Kamarauskaitė Jr, Würth-Roderer K,
624 Kast P, et al. Inter-enzyme allosteric regulation of chorismate mutase in *Corynebacterium*
625 *glutamicum*: structural basis of feedback activation by trp. Biochemistry
626 2017;57(5):557-73. https://doi.org/10.1021/acs.biochem.7b01018.
627 [29] Park W, Son HF, Lee D, Kim IK, Kim KJ. Crystal structure and functional characterization of
628 the bifunctional N-(5'-phosphoribosyl)anthranilate
629 isomerase-indole-3-glycerol-phosphate synthase from *Corynebacterium glutamicum*. J
630 Agric Food Chem 2021;69(42):12485-93. https://doi.org/10.1021/acs.jafc.1c05132.
631 [30] Guo H, Wang N, Ding T, Zheng B, Guo L, Huang C, et al. A tRNA Modification-based
632 strategy for Identifying amiNo acid Overproducers (AMINO). Metab Eng 2023;78:11-25.
633 https://doi.org/10.1016/j.ymben.2023.04.012.
634 [31] Baumgart M, Unthan S, Rückert C, Sivalingam J, Grünberger A, Kalinowski J, et al.
635 Construction of a prophage-free variant of *Corynebacterium glutamicum* ATCC 13032
636 for use as a platform strain for basic research and industrial biotechnology. Appl Environ
637 Microbiol 2013;79(19):6006-15. https://doi.org/10.1128/AEM.01634-13.
638 [32] Tauch A, Kirchner O, Löffler B, Götker S, Pühler A, Kalinowski J. Efficient
639 electrotransformation of *Corynebacterium diphtheriae* with a mini-replicon derived from
640 the *Corynebacterium glutamicum* Plasmid pGA1. Curr Microbiol 2002;45(5):362-7.
641 https://doi.org/10.1007/s00284-002-3728-3.
642 [33] Chen Z, Huang J, Wu Y, Wu W, Zhang Y, Liu D. Metabolic engineering of
643 *Corynebacterium glutamicum* for the production of 3-hydroxypropionic acid from
644 glucose and xylose. Metab Eng 2017;39:151-8.
645 https://doi.org/10.1016/j.ymben.2016.11.009.

[34] Niu J, Mao Z, Mao Y, Wu K, Shi Z, Yuan Q, et al. Construction and analysis of an enzyme-constrained metabolic model of *Corynebacterium glutamicum*. Biomolecules 2022;12(10). https://doi.org/10.3390/biom12101499.

[35] Mao Z, Yuan Q, Li H, Zhang Y, Huang Y, Yang C, et al. CAVE: a cloud-based platform for analysis and visualization of metabolic pathways. Nucleic Acids Res 2023;51(W1):W70-W7. https://doi.org/10.1093/nar/gkad360.

[36] Mao Z, Niu J, Zhao J, Huang Y, Wu K, Yun L, et al. ECMpy 2.0: A Python package for automated construction and analysis of enzyme-constrained models. Synth Syst Biotechnol 2024;9(3):494-502. https://doi.org/10.1016/j.synbio.2024.04.005.

[37] Wu W, Zhang Y, Liu D, Chen Z. Efficient mining of natural NADH-utilizing dehydrogenases enables systematic cofactor engineering of lysine synthesis pathway of *Corynebacterium glutamicum*. Metab Eng 2019;52:77-86. https://doi.org/10.1016/j.ymben.2018.11.006.

[38] Li Z, Dong Y, Liu Y, Cen X, Liu D, Chen Z. Systems metabolic engineering of *Corynebacterium glutamicum* for high-level production of 1,3-propanediol from glucose and xylose. Metab Eng 2022;70:79-88. https://doi.org/10.1016/j.ymben.2022.01.006.

[39] Cohen SA, Strydom DJ. Amino acid analysis utilizing phenylisothiocyanate derivatives. Anal Biochem 1988;174(1):1-16. https://doi.org/10.1016/0003-2697(88)90512-X.

[40] Fang X, Lloyd CJ, Palsson BO. Reconstructing organisms in silico: genome-scale models and their emerging applications. Nat Rev Microbiol 2020;18(12):731-43. https://doi.org/10.1038/s41579-020-00440-4.

[41] Varma A, Boesch BW, Palsson BO. Biochemical production capabilities of *Escherichia coli*. Biotechnol Bioeng 1993;42(1):59-73. https://doi.org/10.1002/bit.260420109.

[42] Ikeda M, Katsumata R. Tryptophan production by transport mutants of *Corynebacterium glutamicum*. Biosci Biotechnol Biochem 2014;59(8):1600-2. https://doi.org/10.1271/bbb.59.1600.

[43] O'Gara JP, Dunican LK. Mutations in the trpD gene of *Corynebacterium glutamicum* confer 5-methyltryptophan resistance by encoding a feedback-resistant anthranilate phosphoribosyltransferase. Appl Environ Microbiol 1995;61(12):4477-9. https://doi.org/10.1128/aem.61.12.4477-4479.1995.

[44] Caligiuri MG, Bauerle R. Identification of amino acid residues involved in feedback regulation of the anthranilate synthase complex from *Salmonella typhimurium.* Evidence for an amino-terminal regulatory site. J Biol Chem 1991;266(13):8328-35. https://doi.org/10.1016/s0021-9258(18)92979-0.

[45] Ikeda M. Towards bacterial strains overproducing l-tryptophan and other aromatics by metabolic engineering. Appl Microbiol Biotechnol 2006;69(6):615-26. https://doi.org/10.1007/s00253-005-0252-y.

[46] Kikuchi Y, Tsujimoto K, Kurahashi O. Mutational analysis of the feedback sites of phenylalanine-sensitive 3-deoxy-D-arabino-heptulosonate-7-phosphate synthase of *Escherichia coli*. Appl Environ Microbiol 1997;63(2):761-2. https://doi.org/10.1128/aem.63.2.761-762.1997.

[47] Peters-Wendisch P, Netzer R, Eggeling L, Sahm H. 3-Phosphoglycerate dehydrogenase from *Corynebacterium glutamicum* : the C-terminal domain is not essential for activity

690 but is required for inhibition by L-serine. Appl Microbiol Biotechnol 2002;60(4):437-41.
691 https://doi.org/10.1007/s00253-002-1161-y.
692 [48] Ikeda M, Nakanishi K, Kino K, Katsumata R. Fermentative production of tryptophan by a
693 stable recombinant strain of *Corynebacterium glutamicum* with a modified
694 serine-biosynthetic pathway. Biosci Biotechnol Biochem 2014;58(4):674-8.
695 https://doi.org/10.1271/bbb.58.674.
696 [49] Jun KH, Jang JH, Rim GG, Lee GC, Huang R, Pyo HH. An L-tryptophan-producing
697 microorganism and methods to use it for L-tryptophan production. CN 105143440 A.
698 2015.
699 [50] Wang J, Zhang R, Zhang J, Gong X, Jiang T, Sun X, et al. Tunable hybrid carbon
700 metabolism coordination for the carbon-efficient biosynthesis of 1,3-butanediol in
701 *Escherichia coli*. Green Chem 2021;23(21):8694-706.
702 https://doi.org/10.1039/d1gc02867g.
703 [51] Dele-Osibanjo T, Li Q, Zhang X, Guo X, Feng J, Liu J, et al. Growth-coupled evolution of
704 phosphoketolase to improve l-glutamate production by *Corynebacterium glutamicum*.
705 Appl Microbiol Biotechnol 2019;103(20):8413-25.
706 https://doi.org/10.1007/s00253-019-10043-6.
707 [52] Lv Q, Hu M, Tian L, Liu F, Wang Q, Xu M, et al. Enhancing l-glutamine production in
708 *Corynebacterium glutamicum* by rational metabolic engineering combined with a
709 two-stage pH control strategy. Bioresour Technol 2021;341:125799.
710 https://doi.org/10.1016/j.biortech.2021.125799.
711 [53] Wray LV, Fisher SH. Functional roles of the conserved Glu304 loop of *Bacillus subtilis*
712 glutamine synthetase. J Bacteriol 2010;192(19):5018-25.
713 https://doi.org/10.1128/jb.00509-10.
714 [54] McHardy AC, Tauch A, Rückert C, Pühler A, Kalinowski J. Genome-based analysis of
715 biosynthetic aminotransferase genes of *Corynebacterium glutamicum*. J Biotechnol
716 2003;104(1):229-40. https://doi.org/10.1016/S0168-1656(03)00161-5.
717 [55] Marienhagen J, Kennerknecht N, Sahm H, Eggeling L. Functional analysis of all
718 aminotransferase proteins inferred from the genome sequence of *Corynebacterium*
719 *glutamicum*. J Bacteriol 2005;187(22):7639-46.
720 https://doi.org/10.1128/jb.187.22.7639-7646.2005.
721 [56] Kurpejović E, Burgardt A, Bastem GM, Junker N, Wendisch VF, Sariyar Akbulut B.
722 Metabolic engineering of *Corynebacterium glutamicum* for l-tyrosine production from
723 glucose and xylose. J Biotechnol 2023;363:8-16.
724 https://doi.org/10.1016/j.jbiotec.2022.12.005.
725 [57] Shang X, Zhang Y, Zhang G, Chai X, Deng A, Liang Y, et al. Characterization and
726 molecular mechanism of AroP as an aromatic amino acid and histidine transporter in
727 *Corynebacterium glutamicum*. J Bacteriol 2013;195:5334-42.
728 https://doi.org/10.1128/JB.00971-13.
729